Influence of Insulation Placement on the Hygrothermal Performance of Hemp Concrete Walls

Ibtissam Asmine [1*], *M'barek Feddaoui* [1], *Lahcen Bammou*[2]

[1]LGEMS Laboratory, National School of Applied Sciences, Ibn Zohr University, Agadir, Morocco

[2]Thermodynamics and Energetic Laboratory, Faculty of Sciences, Agadir, Morocco.

Abstract. This study develops a coupled heat air moisture (HAM) model to assess the hygrothermal response of bio-based porous materials used in building envelopes. The numerical framework was first verified against HAMSTAD benchmark cases that explicitly account for the influence of air transport on moisture migration. The predicted fields show good agreement with the reference solutions, supporting the accuracy of the proposed implementation. The validated model was subsequently applied to a multilayer wall assembly integrating hemp concrete as a bio-based insulating layer. Temperature and relative humidity distributions were evaluated as a function of time and position across the wall under representative summer boundary conditions for Agadir, Morocco, characterized by a hot and dry climate. The simulations indicate that hemp concrete attenuates temperature fluctuations and moderates moisture variations within the envelope, which can contribute to improved indoor comfort and reduced moisture-related risks. Overall, the findings underline the suitability of hemp concrete as an energy efficient and durable insulation material for warm climates and highlight the added value of locally available bio-based resources for enhancing building environmental performance.

1 Introduction

Buildings are a major driver of energy use and greenhouse-gas emissions worldwide, representing a substantial share of final energy demand and CO_2 releases. In Morocco, the building sector accounted for approximately 25% of national energy consumption over the period 2007–2017, with about 18% attributed to residential buildings and 7% to the services sector [1]. Enhancing building energy performance is therefore a strategic priority, not only to reduce consumption but also to improve indoor comfort and limit environmental impacts. Because the envelope governs exchanges between indoor and outdoor environments, the

* Corresponding author: Ibtissamasmine98@gmail.com

selection of construction and insulation materials plays a central role in controlling both thermal behavior and moisture dynamics.

Nomenclature

Latin letters

C_p	specific heat of material (J/kg.K)
g	flow of moisture (kg/m^2.s)
K_l	liquid water permeability (s)
$l_{l;v}$	latent heat (J/kg)
P_a	air pressure (Pa)
P_c	capillary pressure (Pa)
P_{sat}	saturated water vapor pressure (Pa)
P_v	partial water vapor pressure (Pa)
q	heat flow (W/m^2)
t	time (s)
T	temperature (K)
T_{eq}	equivalent temperature (K)
w	moisture content in mass of volume (kg/m^3)
r_a	density of air flow rate (m/s)

Greek letters

α	surface heat transfer coefficient (W/m^2 .K)
β_p	surface vapor transfer coefficient (kg/m^2 .s. Pa)
δ_p	water vapor permeability (kg/m. s. Pa)
λ	thermal conductivity (W/m. K)
ρ	density of material (kg/m^3)

Subscript

a	air
e	exterior side of building envelope
h	heat
i	interior side of building envelope
l	liquid
m	moisture
n	normal direction
surf	surface
sat	saturation state
w	water
v	vapor

Under variable climatic conditions, the coupled transfer of heat, air, and moisture (HAM) becomes particularly important, since these mechanisms interact and jointly determine the hygrothermal response of wall assemblies and the resulting indoor conditions [2,3]. Moisture accumulation and air leakage can degrade thermal comfort, reduce indoor air quality, compromise occupant health, and accelerate material deterioration [4,5]. Airflow through porous or leaky components transports sensible heat and water vapor, thereby modifying local temperature and vapor-pressure gradients and, in turn, influencing moisture redistribution and energy demand [5,6]. In addition, elevated humidity levels and vapor migration can adversely affect the indoor environment and may promote biological contamination and related risks [7].

A growing body of research has investigated HAM processes in building envelopes. Lui Rong et al. compared insulated and non-insulated wall systems incorporating external expanded polystyrene (EPS), using temperature, relative humidity, and air pressure as driving potentials, and reported that external insulation reduces indoor temperature fluctuations and cooling requirements [8]. Steeman et al. developed a three-dimensional model for heat and water-vapor transport in porous media within a CFD framework that accounts for indoor air distribution; validation against measurements demonstrated its ability to predict relative-

humidity variations and evaluate moisture-related risks [9]. Ferroukh et al. introduced the HAM-BES platform, which dynamically couples hygrothermal transfer in multilayer walls with a whole-building thermal model; experimental validation showed that HAM coupling can significantly affect indoor hygrothermal conditions and energy use [10]. Kalamees et al. analyzed pressure differences in Finnish dwellings using measurements and simulations, highlighting the influence of wind and airtightness and underscoring the need for integrated envelope HVAC design, particularly in low-energy buildings [11]. Dong et al. examined the influence of air infiltration on indoor air quality, envelope performance, and energy consumption, and compared several modeling approaches to support improved design and operation strategies [12]. Delgadillo Buenrostro et al. further demonstrated that airflow across envelope components especially at wall junctions could substantially modify temperature and humidity fields, emphasizing the necessity of explicitly representing air transport in hygrothermal simulations to better reflect real building behavior [13].

A growing body of research has investigated HAM processes in building envelopes, using both experimental and numerical approaches. Several studies have demonstrated the importance of coupling heat and moisture transfer for predicting hygrothermal behavior, while others have emphasized the role of air infiltration and pressure-driven airflow in modifying temperature and humidity fields. However, most existing works focus either on conventional insulation materials or on heat and moisture transfer without fully accounting for the interaction between air transport, insulation placement, and bio-based materials. In particular, the influence of insulation location (internal versus external) on the coupled heat–air–moisture behavior of hemp-concrete wall assemblies under hot and dry climatic conditions remains insufficiently investigated.

This study examines the integration of hemp concrete into multilayer wall assemblies and investigates its capacity to regulate temperature and humidity under summer conditions in Agadir, Morocco, a region characterized by a hot and dry climate. The numerical model is first validated against HAMSTAD benchmark cases to assess the influence of air transport on moisture behavior. It is then applied to analyze the hygrothermal performance of several hemp-concrete wall configurations, with particular emphasis on the role of insulation placement in thermal inertia, heat transfer, and moisture redistribution. By addressing this design issue, the study contributes to the evaluation of hemp concrete as a sustainable and energy-efficient material for buildings in warm climates.

2 Modeling

2.1 Coupled heat and moisture transfer equations

The model is developed under the following assumptions [3]:

- Effects related to phase changes from liquid to ice are neglected.
- Hysteresis is not considered.
- Chemical reactions are not taken into account.
- Ageing effects and changes in geometrical dimensions are neglected.
- The impact of driving rain is simplified in the climatic load.

2.1.1 Moisture transfer

Moisture transfer is divided into vapour and liquid flow.

$$g = g_l + g_{v,d} \quad (1)$$

The liquid flow is described as follows:

$$g_l = K.\frac{dP_{suc}}{dx} \quad (2)$$

The liquid water permeability, K, varies with moisture content and temperature. Vapour transport occurs through a combination of diffusion and convection.

$$g_{v,d} = -\delta_p.\frac{dP}{dx} + r_a \upsilon_a \quad (3)$$

In the diffusive component, $\boldsymbol{\delta_p}$ represents the vapor permeability, which varies with moisture content. In the convective component, $\boldsymbol{\upsilon_a}$ denotes the water vapor content, also referred to as volumetric humidity.

2.1.2 Heat transfer

Heat transfer occurs through two mechanisms. One part is conductive, while the other is convective.

$$q = q_{cond} + q_{conv} \quad (4)$$

The conductive component of heat transfer is described by the following expression. It represents the heat flux resulting from conduction within the material.

$$q_{cond} = -\lambda\frac{dT}{dx} \quad (5)$$

Here, $\boldsymbol{\lambda}$ represents the thermal conductivity, which varies with local moisture content and temperature. The convective component of heat transfer is expressed as:

$$q_{conv} = r_a \rho_a c_{p,a} T + g_v l_{lv} \quad (6)$$

The specific heat capacity, $c_{p,a}$, corresponds to humid air. The second term represents the contribution of latent heat.

2.1.3 Energy and moisture balance

The energy balance equation

$$-\frac{\partial q}{\partial x} = c\rho_0\frac{\partial T}{\partial t} \quad (7)$$

$$\frac{\partial}{\partial x}\left(\lambda\frac{\partial T}{\partial x}\right) - r_a\rho_a c_{p,a}\frac{\partial T}{\partial x} + l_{lv}\frac{\partial}{\partial x}\left(\delta_p\frac{\partial p}{\partial x}\right) - r_a l_{lv}\frac{\partial \upsilon}{\partial x} = c\rho_0\frac{\partial T}{\partial t} \quad (8)$$

The mass balance equation

$$-\frac{\partial g}{\partial x} = \frac{\partial w}{\partial t} \quad (9)$$

$$\frac{\partial}{\partial x}\left(\delta_p \frac{\partial p}{\partial x}\right) - r_a \frac{\partial v}{\partial x} - \frac{\partial}{\partial x}\left(K.\frac{dP_{suc}}{dx}\right) = \frac{\partial w}{\partial t} \quad (10)$$

2.1.4 Boundary conditions

The total moisture flux, including vapour transport, g_v, is given by:

$$g_v = \pm\beta_p\left(p_a - p_{surf}\right) + r_a v_a \quad \text{air entering the surface} \quad (11)$$

$$g_v = \pm\beta_p\left(p_a - p_{surf}\right) + r_a v_{surf} \quad \text{air exiting the surface} \quad (12)$$

The subscript a refers to ambient conditions. A positive sign is applied at the surface with the lowest x-coordinate, while a negative sign corresponds to the surface with the highest x-coordinate. It is important to note that r_a is positive when the flux is directed along the positive x-axis.

The heat flux, q, from the ambient to the surface, accounting for inflow of air and liquid water, is given by:

$$q_n = \pm\alpha_e\left(T^{eq} - T_{surf}\right) + r_a \rho_a c_{p,a+v} T_a + g_l c_{p,l} T_a + g_v l_{l;v} \quad (13)$$

In the case of air outflow without liquid water inflow:

$$q_n = \pm\alpha_e\left(T^{eq} - T_{surf}\right) + r_a \rho_a c_{p,a+v} T_{surf} + g_v l_{l;v} \quad (14)$$

The surface film coefficient,α_e, incorporates both convective heat transfer and long-wave radiation. The equivalent temperature, T_{eq}, combines the effects of air temperature, solar radiation, and long-wave radiative exchange. A positive sign indicates the surface with the lowest x-coordinate, whereas a negative sign corresponds to the surface with the highest x-coordinate.

Indoor temperature and relative humidity were imposed as constant boundary conditions representative of typical summer comfort conditions. Moisture generation associated with occupants or indoor activities was not considered, in order to focus on the inherent hygrothermal behavior of the wall assembly. Airflow through the envelope was represented by a pressure-driven term accounting for ventilation and wind effects.

Heat exchange at the wall surfaces was modeled using a wind-dependent convective heat transfer coefficient. Wind-driven rain was neglected, as the analysis was restricted to summer conditions in a hot and dry climate where liquid moisture loads are minimal.

3 Model validation

3.1 Cas 1

This study used HAMSTAD Benchmark Case 2 to validate the model. The benchmark considers moisture redistribution in a homogeneous single-layer wall under isothermal conditions. The wall thickness is 200 mm. The interior and exterior boundary conditions are set at 293 K with relative humidities of 65% and 45%, respectively, while the initial

conditions are 293 K and 85% relative humidity. The heat and mass transfer coefficients are 25 W/(m²·K) and 1 × 10^{-3} s/m. The simulation was run for 1000 hours. **Figure 2** shows the moisture content [kg/m³] across the wall thickness at 100, 300, and 1000 hours [14].

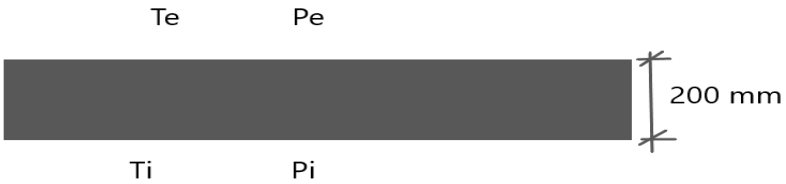

Fig. 1. Schematic of the structure of benchmark.

3.2 Cas 2

Benchmark 3, developed by Chalmers University of Technology (CTH) as part of the HAMSTAD project, is a 1D tool for verifying coupled heat, air, and moisture (HAM) models. It provides reference solutions from participating universities to check the accuracy and consistency of numerical simulations. The benchmark considers a homogeneous wall layer initially at steady state, with both sides at 20°C and 95% relative humidity.
At time zero, indoor relative humidity drops to 70%, outdoor humidity rises to 80%, indoor temperature stays at 20°C, and outdoor temperature decreases to 2°C. The model represents a 200 mm lightweight wall exposed to air exfiltration for the first 20 days and air infiltration over the next 80 days, see **Figures (3, 4)**. Moisture transfer is driven mainly by airflow and also by temperature and humidity differences. The exterior face is vapor-tight but allows air to pass. Convective heat and moisture transport was simulated by applying a pressure difference of ±30 Pa between the interior and exterior, leading to alternating phases of air infiltration and exfiltration [14].

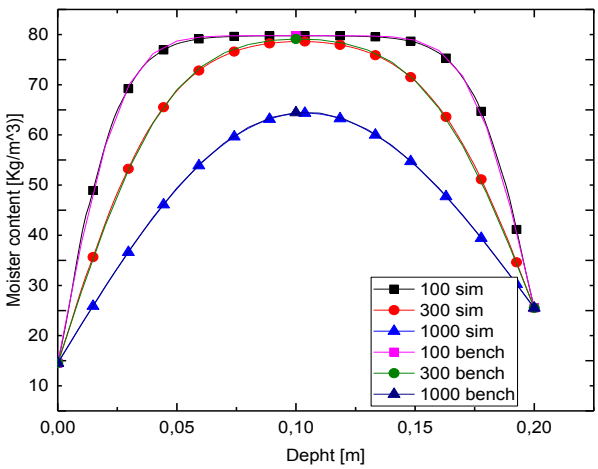

Fig. 2. Average moisture content within the insulation

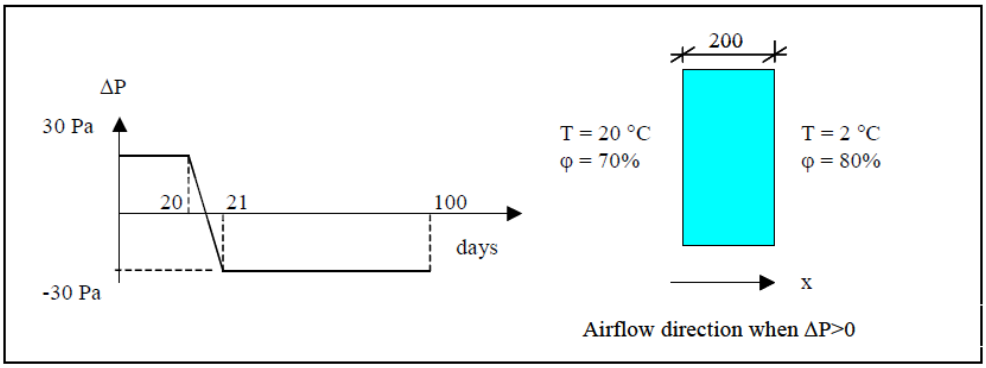

Fig. 3. Light-weight wall and the air filtration strategy.

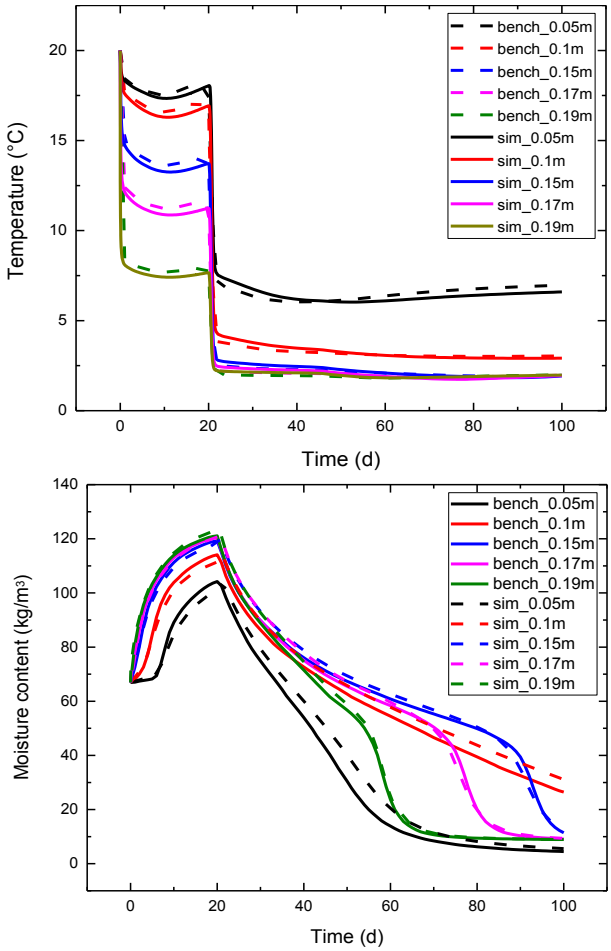

Fig. 4. Temperature and moisture variations over time in different wall sections with air infiltration.

The root mean square error (RMSE) was employed to assess the difference between the simulated and reference values, offering an objective evaluation of the numerical model's accuracy.

$$RMSE = \left[\frac{\sum_{i=1}^{n}(X_i - X_i)^2}{n}\right]^{1/2} \quad (15)$$

Table 1. RMSE of temperature and moisture content during model validation.

Position (X)	RMSE [Temperature (°C)]	RMSE [Moisture content (kg/m3)]
0.05 m	1.03099	1.95
0.1 m	1.42	1.179

4 Case Study: Hygrothermal Performance of Hemp Concrete

4.1 Configuration of the wall

In this study, we investigate the hygrothermal behaviour of a red brick wall insulated with hempcrete. Three wall configurations are considered: a configuration with insulation applied on the interior side**, see Figure 6(a)**, a configuration with insulation applied on the exterior side**, see Figure 6(b)** and a reference configuration without insulation**, see Figure 5**. The wall structure is the same in both cases, only the location of the insulation layer changes. From the exterior to the interior, the wall consists of a 2 cm lime plaster, a 20 cm red brick layer, 10 cm of hempcrete, and a 1.5 cm interior lime plaster.

The simulations are carried out under summer weather conditions typical of Agadir. Indoors, the temperature is fixed at 20 °C and the relative humidity at 45%. The outdoor boundary conditions follow the usual daily summer pattern observed in Agadir, **see Figure 7**. Air movement is also included in the analysis, taking into account ventilation and the local wind speed characteristic of this coastal region. The material properties are obtained from [15] (show in **Table 2**).

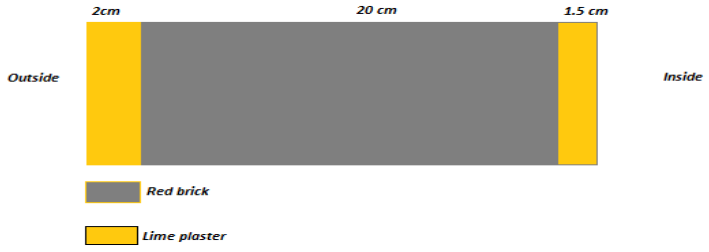

Fig. 5. Uninsulated red brick wall

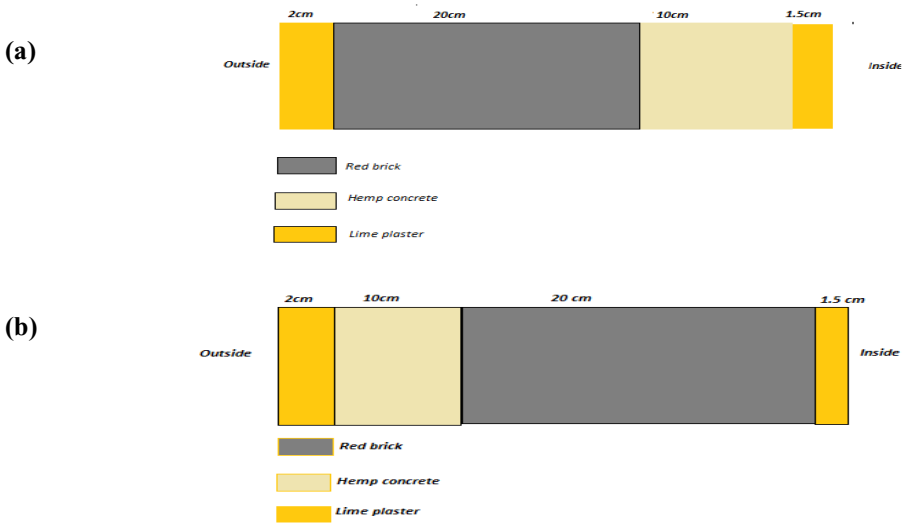

Fig. 6. Configuration of the two wall systems: Wall a (interior hemp concrete insulation) and Wall b (exterior hemp concrete insulation)

v

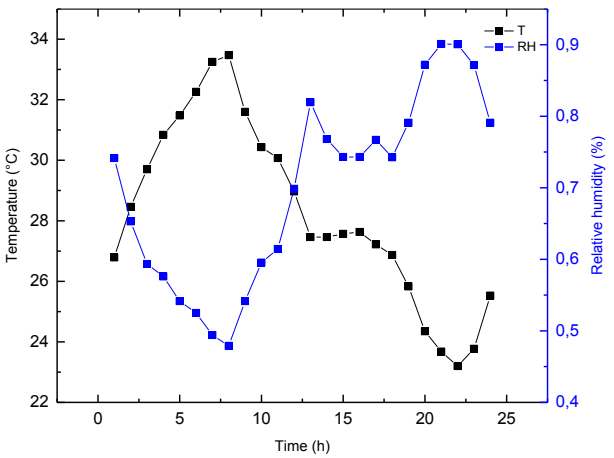

Fig.7.Climatic conditions of temperature and relative humidity in Agadir during summer

Table2. Properties of the wall components [15].

Properties	**Hemp concrete**	**Brick**	**Lime-cement plaster**
Thermal conductivity $(W/m\,K)$	0.11	$-6.72.10-6\,T^2+1.83.103T+0.37$	$\phi/(0.00674\phi^{20.0135}\phi+0.0077)$
Specific heat capacity $(J/kg\,K)$	1000	$-3.88.1017T^2+1.323T+697.6$	1050
Density (kg/m^3)	390	1847	1600
Water vapor permeability (s)	$2.5.10^{-11}$	$1.4342.\,10^{-12}$	$1.2/10^{-11}$

4.2 Results and discussion

The influence of insulation location on the wall response under coupled heat–air–moisture (HAM) transfer was evaluated by comparing three assemblies: hemp-concrete insulation placed on the interior side, on the exterior side, and a reference wall without insulation. The discussion below focuses on the interior-side temperature and relative humidity histories shown in **Figures (8**, **9)**.

From a thermal perspective (Fig. 8), the three cases display a brief start-up phase with a rapid rise in interior temperature, followed by a quasi-steady regime. The internally insulated configuration reaches the lowest stabilized interior temperature (≈ 20.2 °C), which is consistent with a reduced contribution of the wall mass to heat storage when insulation is located on the room side. With external insulation, the stabilized interior temperature is slightly higher (≈ 20.3 °C), reflecting the greater effective thermal inertia of the protected wall, which dampens the propagation of outdoor thermal loads toward the indoor environment. In contrast, the uninsulated wall exhibits the highest interior temperature level (≈ 20.6 °C), indicating a stronger coupling between the indoor side and the wall mass, and thus a larger net heat transfer through the envelope.

The moisture response at the interior surface (Fig. 9) follows a similar pattern for all configurations: the relative humidity starts near 45% and decreases sharply during the first hours, corresponding to the hygric adjustment of the wall to the imposed boundary conditions. The uninsulated wall undergoes the most pronounced drop and stabilizes at the lowest level (≈ 43.3 – 43.4% after ~250 h), suggesting more effective moisture exchange with the exterior environment. Adding insulation limits this exchange and leads to higher stabilized indoor-side humidity. With external insulation, the interior relative humidity stabilizes earlier around 44.1 – 44.2%, while the wall layers retain a moderate buffering role. With internal insulation, the interior relative humidity remains slightly higher at long times (≈ 44.3 – 44.4%), consistent with reduced moisture interaction between the indoor air and the underlying masonry, which slows redistribution within the assembly.

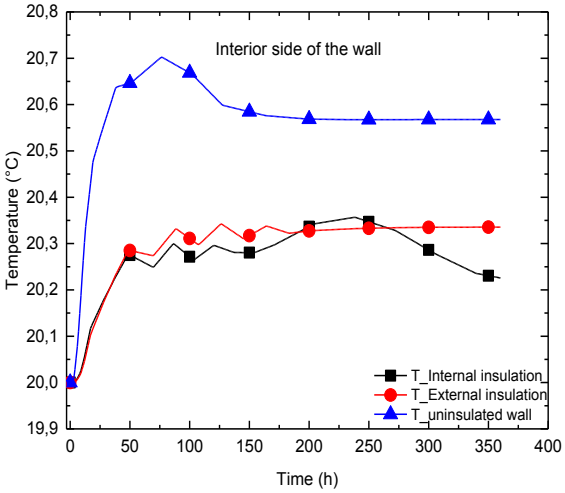

Fig. 8. Variations in the interior temperature.

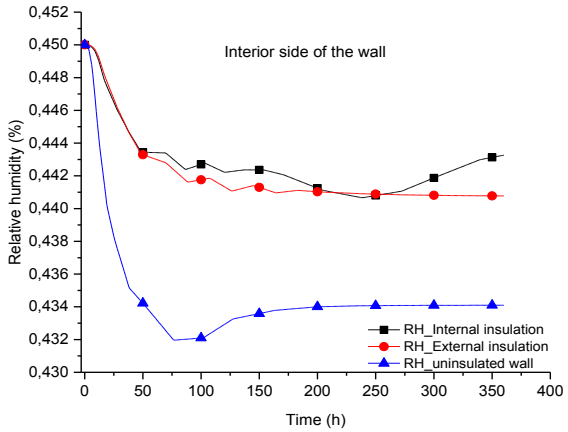

Fig. 9. Variations in the interior relative humidity

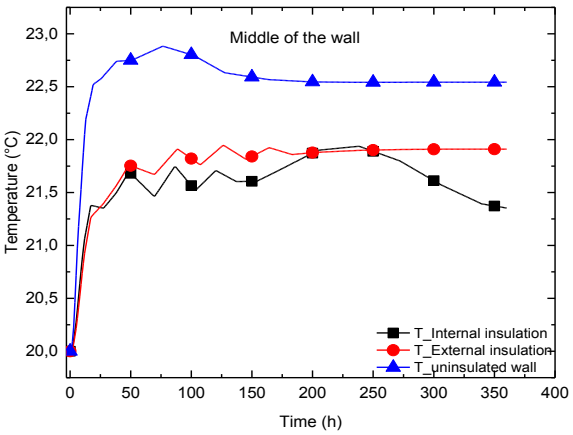

Fig. 10. Temperature variations at the mid-wall section

Figure 10. presents the time-dependent temperature response at the wall mid-depth for the three assemblies. In all cases, a short start-up period is observed, during which the core temperature rises rapidly as the wall adjusts to the prescribed indoor outdoor boundary conditions. The uninsulated wall shows the warmest mid-plane response, with an early peak close to 22.8 °C followed by a quasi-steady level of approximately 22.5 – 22.6 °C. This behavior is expected because, without an insulating layer, the exterior thermal load is transmitted more efficiently into the wall thickness.

When insulation is placed on the exterior, the mid-plane temperature remains noticeably lower and stabilizes around 21.9 – 22.0 °C, indicating that the hemp-concrete layer reduces the incoming heat flux and better protects the structural core from outdoor heating. The internally insulated configuration yields the lowest temperatures at mid-depth (about 21.4 – 21.5 °C), with a slight decrease toward the end of the simulation. This trend reflects a stronger thermal separation of the wall mass from the interior side, which limits heat storage within the wall core and alters the direction and magnitude of heat exchange across the assembly.

Figure 11 depicts the time evolution of relative humidity at the wall mid-depth for the three configurations. All cases show a pronounced decrease during the early hours, which

corresponds to the hygric equilibration of the assembly with the imposed boundary conditions. The uninsulated wall exhibits the strongest drop and reaches the lowest quasi-steady values (approximately 43.1–43.3%), indicating more intense moisture exchange with the exterior and a greater drying potential within the wall core.
Introducing insulation mitigates this response. With external insulation, the mid-wall relative humidity stabilizes at slightly higher levels (about 44.0–44.1%), consistent with reduced exposure of the structural layer to outdoor vapor-pressure variations while maintaining a limited buffering capacity. The internally insulated case yields the highest mid-depth humidity (roughly 44.1–44.2%), suggesting that moisture redistribution is more constrained and that the core retains moisture for longer periods when the insulation is placed on the room side.
Overall, insulation placement significantly influences moisture regulation within the wall core: external insulation tends to smooth the hygric response and promote stabilization, whereas internal insulation leads to marginally higher retained moisture. In contrast, the absence of insulation accelerates drying but may increase the risk of moisture-related deterioration through larger hygric gradients and more pronounced exchanges with the outdoor environment.

Figure 12.presents the temporal evolution of the exterior-surface temperature for the three wall assemblies. Immediately after the beginning of the simulation, all cases show a sharp temperature rise, which reflects the rapid adjustment of the external surface to the imposed outdoor boundary conditions (thermal step change). During the first hours, clear differences appear between configurations: both internally and externally insulated walls exhibit higher surface temperature peaks (on the order of 30–31 °C) than the uninsulated wall. This response is consistent with the increased thermal resistance introduced by insulation, which reduces heat transmission toward the inner layers and therefore promotes short-term heat build-up at the outer surface. By contrast, the uninsulated wall enables a larger portion of the absorbed heat to be redistributed through the wall thickness, limiting the magnitude of the surface peak.

After the transient period, the curves converge toward a quasi-steady regime in which exterior surface temperatures become very close for the three configurations. This indicates that, at longer times, the exterior temperature is governed primarily by the outdoor environment, while insulation placement has only a secondary influence on the external surface condition.

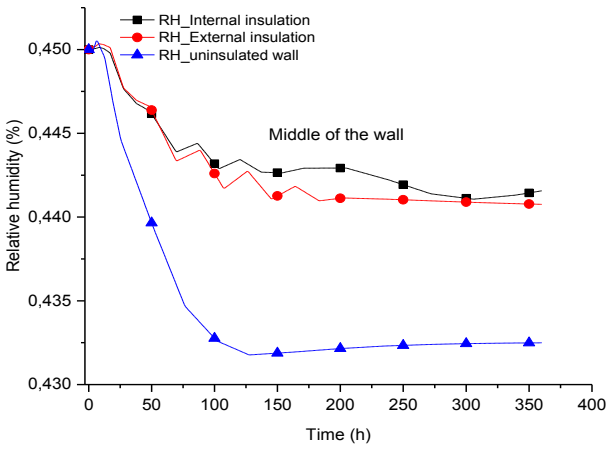

Fig. 11. Relative humidity variations at the mid-wall section

Figure 13 illustrates the time evolution of relative humidity at the exterior surface for the three wall configurations. At the start of the simulation, the curves are close to one another and exhibit small short-term oscillations, which are attributable to the initial adjustment of the surface to the imposed outdoor climatic boundary conditions. After this transient phase, the responses diverge.

The uninsulated wall shows a modest decrease followed by a nearly steady plateau around 43%, indicating that the exterior-surface humidity is primarily governed by the outdoor environment when no insulating layer alters moisture transport. For the externally insulated assembly, the exterior relative humidity decreases progressively and remains slightly below the uninsulated case. This trend suggests that the external insulation modifies vapor diffusion pathways and partially limits moisture exchange at the outer boundary. In contrast, the wall with internal insulation exhibits the largest reduction in exterior relative humidity, approaching 40% at longer times, which is consistent with enhanced drying of the outer layer when the insulation is placed on the interior side and the exterior zone remains more directly exposed to hygric driving forces.

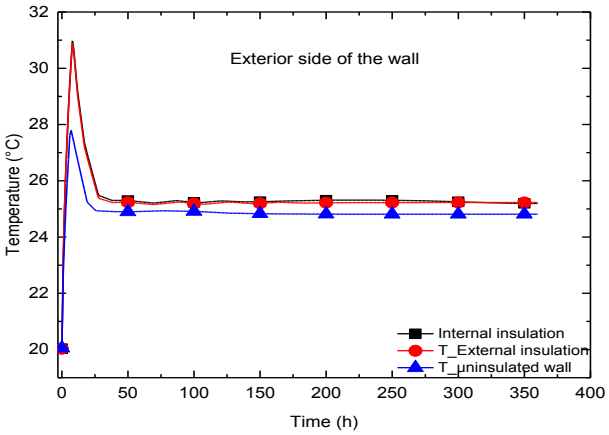

Fig. 12. Evolution of exterior relative humidity

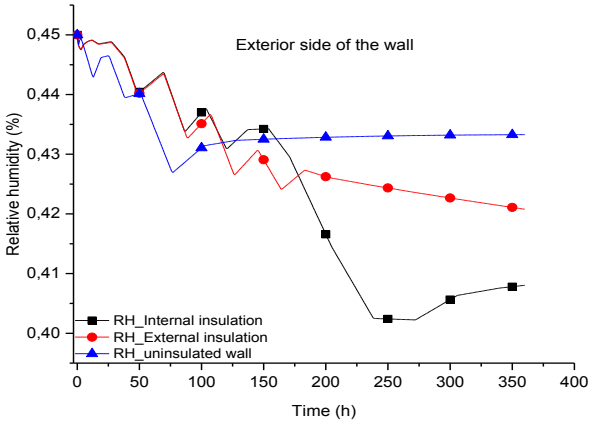

Fig. 13. Evolution of exterior temperature.

Overall, the results show that where you place the insulation doesn't just change what happens inside the wall it also affects how the outside surface behaves. With internal insulation, the outer part of the wall tends to dry out more, while external insulation keeps moisture levels steadier by protecting the wall from direct outdoor effects.

Monitoring the state variables at multiple depths shows that the hygrothermal response of the wall is largely controlled by the presence of hemp concrete and, more importantly, by its location within the assembly under Agadir summer conditions. The non-insulated wall is the most directly influenced by the outdoor boundary, exhibiting higher heat transfer across the section and larger moisture fluctuations, which reflect a limited buffering capacity. Introducing a hemp-concrete layer reduces conductive heat penetration and modifies vapor transport by damping temperature variations and, consequently, the associated vapor-pressure gradients. When the insulation is placed on the interior side, the contribution of the wall core to heat storage decreases and moisture tends to remain closer to the indoor layer, resulting in a slight increase in interior-side relative humidity. In contrast, external hemp-concrete insulation protects the structural mass, increases the effective thermal inertia, attenuates temperature oscillations, and promotes a more homogeneous and stable moisture profile by reducing the influence of outdoor forcing. Overall, the results suggest that hemp concrete can be a practical, bio-based insulation option for hot, dry climates: it helps keep indoor conditions more comfortable, limits moisture problems, and can support longer lasting wall assemblies. At the same time, the study makes it clear that the final performance depends strongly on where the insulation is placed, so placement should be treated as a key design choice.

5 Conclusion

In this work, we looked at how hemp-concrete insulation changes the way a wall exchanges heat, air, and moisture when the insulation is placed in different positions. We first checked that our simulation approach was trustworthy by comparing it with two well-known HAMSTAD benchmark cases, where heat and moisture move together with airflow. After this verification step, we used COMSOL Multiphysics to model a multilayer wall that includes hemp concrete and is exposed to typical summer conditions in Agadir (Morocco). We followed how temperature and relative humidity evolve over time at three key locations: the inside surface, the wall core, and the outside surface. The main message is clear: where the insulation is placed matters a lot, because it changes how much heat the wall can store and how moisture is redistributed through the layers. Overall, hemp concrete helped smooth temperature swings and limit moisture transfer, which supports better indoor comfort and could also improve the long-term durability of wall materials in hot, dry climates.

References

1. AMEE, Règlement thermique de construction au Maroc (RTCM), Agence Marocaine pour l'Efficacité Énergétique (2013).
2. M. Dlimi, R. Agounoun, I. Kadiri, R. Saadani, M. Rahmoune, Thermal performance assessment of double hollow brick walls filled with hemp concrete insulation material through computational fluid dynamics analysis and dynamic thermal simulations. *e-Prime* **3**, 100124 (2023).

3. C.-E. Hagentoft, B. Adl-Zarrabi, O. C. G. Adan, R. Becker ,Assessment Method of Numerical Prediction Models for Combined Heat, Air and Moisture Transfer in Building Components : Benchmarks for One-Dimensional Cases. Build. Phys. (2004).
4. S.-S. Chua, T.-H. Fang, W.-J. Chang, Modelling of coupled heat and moisture transfer in porous construction materials. Math. Comput. Model.**50**, 1195–1204 (2009).
5. U. Mathur, R. Damle, Impact of air infiltration rate on the thermal transmittance value of building envelope. J. Build. Eng.**40**, 102302 (2021).
6. J. Jokisalo, J. Kurnitski, M. Korpi, T. Kalamees, J. Vinha, Building leakage, infiltration, and energy performance analyses for Finnish detached houses. Build. Environ.**44**, 377–387 (2009).
7. S. Shetty, P. Kishore, P. Kini, R. R. Acharya, A. Raj, Energy Conservation Building Code (ECBC) based optimum wall composition with respect to thermal transmittance and thickness for different commercial pockets of Tier-1 city in temperate climatic zone of India. Procedia. Manuf.**44**, 229–236 (2020).
8. R. Liu, Y. Huang, Heat and moisture transfer characteristics of multilayer walls. Energy Procedia.**152**, 324–329 (2018).
9. H.-J. Steeman, M. Van Belleghem, A. Janssens, M. De Paepe, Coupled simulation of heat and moisture transport in air and porous materials for the assessment of moisture related damage. Build. Environ. **44**, 2176–2184 (2009).
10. M. Y. Ferroukhi, R. Djedjig, R. Belarbi, K. Limam, K. Abahri, Effect of coupled heat, air and moisture transfers modeling in the wall on the hygrothermal behavior of buildings. *Energy Procedia* .**78**, 2584–2589 (2015).
11. T. Kalamees, J. Kurnitski, J. Jokisalo, J. Vinha, Measured and simulated air pressure conditions in Finnish residential buildings. Build. Serv. Eng. Res. Technol. **31**, 177–190 (2010).
12. W. Dong, Y. Liu, Y. Wang, X. Mei, Comprehensive analysis and evaluation of air infiltration prediction models in building envelopes. *J. Build. Eng.* **99**, 111520 (2025)
13. L. Delgadillo Buenrostro, L. Gosselin, P. Blanchet, Hygrothermal response to air movements in wall junctions: Comparison between two numerical approaches and experiments. Int. J. Therm. Sci. **203**, 109169 (2024).
14. A. W. M. van Schijndel, S. Goesten, H. L. Schellen, Simulating the complete HAMSTAD benchmark using a single model implemented in COMSOL. *Energy Procedia*.**132**, 429–434 (2017).
15. X. Liu, Y. Chen, H. Ge, P. Fazio, G. Chen, Numerical investigation for thermal performance of exterior walls of residential buildings with moisture transfer in hot summer and cold winter zone of China. Energy Build.**93**, 259–268 (2015).